Inorg. Chem. **2008**, *47*, 3408−3414

Synthesis and Photophysical Properties of Ruthenium-Based Dendrimers and Their Use in Dye Sensitized Solar Cells

Ali H. Younes and Tarek H. Ghaddar*

Department of Chemistry, American University of Beirut, Beirut 11-0236, Lebanon

Received December 17, 2007

First- and second-generation dendrimers (**Ru3** and **Ru6**) have been synthesized, and their photophysical properties were investigated in solution and when adsorbed on the nanocrystalline TiO_2 surface. The performance of **Ru3** and **Ru6** as charge transfer photosensitizers in nanocrytalline TiO_2 based solar cells was also investigated. The best photovoltaic performance was obtained by the **Ru3** based solar cell yielding a short circuit current of $J_{sc} = 5.52\ mA \cdot cm^{-2}$ and an open circuit voltage of $V_{oc} = 626$ mV, corresponding to an overall conversion efficiency of $\eta = 1.80\%$ that is approximately double the conversion efficiency of the reference compound **Ru1** ($\eta = 0.91\%$) and of the second generation dendrimer **Ru6** ($\eta = 0.95\%$). The particular efficiency of the first generation dendrimer, **Ru3**, is attributed to the better light-harvesting properties of the doped nanocrystalline TiO_2 film when compared to **Ru1**, whereas the poor performance of the second generation dendrimer, **Ru6**, is attributed to the uneven adsorption of all of the ruthenium moieties to the nanocrystalline TiO_2 surface at the same time.

Introduction

Dendrimers are regarded as excellent candidates for light-harvesting antenna systems as a result of their three-dimensional hyper-branched structure.[1,2] Dendrimers can be synthesized with high numbers of light absorbing or photoactive units at the periphery that can transfer the harvested-light energy through electron- or energy-transfer reactions to a redox active site. With such properties, dendrimers are very attractive synthetic polymers that can be used in the area of conversion of solar energy into electricity.[3–7] However, to take advantage of such properties and to utilize the harvested-light energy for solar photoconversion, electrons should flow to an electrode.[8,9]

In 1991 Grätzel and O'Regan introduced the dye-sensitized solar cell (DSSC) in which a triad dye molecule was anchored to the surface of nanocrystalline TiO_2, and upon visible light excitation an electron is injected from the excited dye to the TiO_2 conduction band.[10] The high conversion efficiency ($\eta = 7.12\%$) of the triad dye was attributed to its high light harvesting ability. Since then, ruthenium polypyridyl based dyes have received great attention as a result of their promising performance as sensitizers,[11–16] where DSSC efficiencies of up to 11% have been reached.[17] On the other hand, some organic dye sensitizers[18] and polymer-based

* To whom correspondence should be addressed. Tel.: +961-3-464568. Fax: +961-1-365217. E-mail: tg02@aub.edu.lb.

(1) Newkome, G. R.; He, E. F.; Moorefield, C. N. *Chem. Rev.* **1999**, *99*, 1689–1746.
(2) Bosman, A. W.; Janssen, H. M.; Meijer, E. W. *Chem. Rev* **1999**, *99*, 1665–1688.
(3) Peumans, P.; Yakimov, A.; Forrest, S. R. *J. Appl. Phys.* **2003**, *7*, 3693–3723.
(4) Nelson, J. M. *Curr. Opin. Solid Mater. Sci.* **2002**, *6*, 87–95.
(5) Devadoss, C.; Bharathi, P.; Moore, J. S. *J. Am. Chem. Soc.* **1996**, *118*, 9635–9644.
(6) Adronov, A.; Frechet, J. M. J. *Chem. Commun.* **2000**, 1701–1710.
(7) Balzani, V.; Ceroni, P.; Maestri, M.; Vicinelli, V. *Curr. Opin. Chem. Biol.* **2003**, *7*, 657–665.
(8) Marcus, R. A.; Sutin, N. *Biochim. Biophys. Acta* **1985**, *811*, 265–322.
(9) Ohkita, H.; Ishii, H.; Ogi, T.; Ito, S.; Yamamoto, M. *Radiat. Phys. Chem.* **2001**, *60*, 427–432.
(10) O'Regan, B.; Grätzel, M. *Nature* **1991**, *353*, 737–740.
(11) Islam, A.; Sugihara, H.; Arakawa, H. *J. Photochem. Photobiol. A* **2003**, *158*, 131–138.
(12) Jiang, K. J.; Masaki, N.; Xia, J. B.; Noda, S.; Yanagida, S. *Chem. Commun.* **2006**, 2460–2462.
(13) Islam, A.; Chowdhury, F. A.; Chiba, Y.; Komiya, R.; Fuke, N.; Ikeda, N.; Nozaki, K.; Han, L. *Chem. Mater.* **2006**, *18*, 5178–5185.
(14) Morandeira, A.; Lopez-Duarte, I.; Martinez-Diaz, M. V.; O'Regan, B.; Shuttle, C.; Haji-Zainulabidin, N. A.; Torres, T.; Palomares, E.; Durrant, J. *J. Am. Chem. Soc.* **2007**, *129*, 9250–9251.
(15) Chen, C. Y.; Wu, S. J.; Wu, C. G.; Chen, J. G.; Ho, K. C. *Angew. Chem.* **2006**, *45*, 5822–5825.
(16) Argazzi, R.; Bignozzi, C. A.; Hasselmann, G. M.; Meyer, G. J. *Inorg. Chem.* **1998**, *37*, 4533–4537.
(17) Grätzel, M. *J. Photochem. Photobiol. A* **2004**, *164*, 3–14.
(18) Horiuchi, T.; Miura, H.; Sumioka, K.; Uchida, S. *J. Am. Chem. Soc.* **2004**, *126*, 12218–12219.

10.1021/ic702432u CCC: $40.75
Published on Web 03/06/2008

dyes[19–21] have been developed for DSSCs, giving respectable incident photon to current efficiency (IPCE). To date, *cis*-dithiocyanato-bis(4,4′-dicarboxylic acid-2,2′-bipyridine)ruthenium(II) (N3) has been a paradigm in this field as a result of its outstanding performance. In spite of this, one of the main drawbacks of this sensitizer is the relatively low molar extinction coefficient in the visible and near-IR.[22] To overcome this problem, different strategies have been employed, such as extending the conjugation in the ancillary ligand,[23,24] the use of multichromophoric dyes,[10,25,26] or both.[27]

This led us to the strategy of designing sensitizing dyes with a high light absorption cross-sectional area that incorporates polypyridyl ruthenium(II) complexes in a dendritic architecture. As a model, we synthesized first- and second-generation dendrimers that incorporate polypyridyl ruthenium(II) groups at the periphery. As such, we will be investigating the dendritic effect on the DSSC efficiency which may result in a new strategy to be used in the future for preparing dendritic dyes that contain multi-**N3** analogs at the periphery. Herein, we report the synthesis, photophysical, and photoelectrochemical properties of two dendrimers (**Ru3** and **Ru6**) and compare them to the mononuclear reference compound, $(4,4'\text{-dc-bpy})_2\text{Ru(dm-bpy)}$, **Ru1**.

Experimental Section

Materials and Instrumentation. All organic chemicals were purchased from Aldrich and used as supplied. The solar cell material was purchased from Solaronix (Switzerland). 4-Bromomethyl-4′-methyl-2,2′-bipyridine,[28] $(4,4'\text{-dc-bpy})_2\text{RuCl}_2$,[29] and $[(4,4'\text{-dc-bpy})_2\text{Ru(dm-bpy)}][\text{Cl}_2]$[30] (where dc = dicarboxy, dm = dimethyl, and bpy = 2,2′-bipyridine) were prepared using reported procedures in the literature. Acetone and tetrahydrofuran (THF) were distilled from anhydrous potassium carbonate and sodium/benzophenone prior to use, respectively. Emission spectra were measured on a JobinYvon Horiba Fluorolog-3 spectrofluorometer. The emission quantum yields were measured in Ar saturated solution with use of $\text{Ru(bpy)}_3[\text{PF}_6]_2$ in water as a standard ($\Phi = 0.042$).[31] Time-correlated single photon counting (TCSPC) emission decay measurements were done using an IBH NanoLED-460 diode laser for the excitation source and an IBH TBX-04 photomultiplier detector, and the lifetimes were obtained by curve-fitting with an IBH DAS 6.0 program. The NMR spectra (^{1}H and ^{13}C) were measured on a Bruker AM 300 MHz spectrometer. UV–vis spectra were recorded on a Jasco V-570 UV/vis/NIR. The thickness of the TiO_2 films was measured using Alpha-step 200 profilometer. An Oriel 150 W Xenon lamp (Newport, U.S.A.) was used as the light source in conjunction with a UV and an IR cutoff filter (Edmund Optics, U.S.A.). The light intensity was adjusted to 100 mW/cm^2 by the aid of a neutral density filter (Edmund Optics, U.S.A.). The irradiated area of the cell was 0.120 cm^2. The $I-V$ curves of the solar cells were measured by applying a variable external resistance load, and the current and voltage were measured with a CHI bipotentiostat (model 630).

Solar Cell Preparation. The 8.0 ± 0.2 μm thick films of nanocrystalline TiO_2 were deposited on transparent conducting glass (SnO_2:F, FTO) by the doctor blade squeegee method using a double layer of 3 M scotch tape as the determining thickness spacer and TiO_2 paste (Ti-nanoxide T, Solaronix). The films were then air-dried followed by sintering in an oven at 480 °C for 30 min. After cooling, the TiO_2 films were impregnated in the dye solutions that were prepared in a concentration range of 3–4 × 10^{-4} M (per one ruthenium tris-bipyridine moiety) in 1:1 methanol/water adjusted to pH = 3.5 with dilute HCl. The electrodes were dipped for 24 h, after which the dye-deposited films (working electrodes) were washed with methanol and air-dried. In the fabrication of the dye-sensitized solar cell, the sandwich cell was prepared using a second FTO conducting glass with two predrilled holes for the electrolyte introduction as the counter electrode and was precoated with a thin layer of platinum. The deposition of the platinum layer was accomplished by brushing the FTO conducting glass with a 5 mM H_2PtCl_6 in isopropanol (Platisol, Solaronix), followed by sintering in an oven at 400 °C for 30 min. Using a thin transparent film of Surlyun polymer (Dupont, U.S.A.), the two electrodes were put together and tightly held at 120–130 °C around the surlyun frame in order to seal the cell. Then, through the predrilled holes in the counter electrode side, the electrolyte (Iodolyte MPN-100, Solaronix) consisting of I_2 0.05 M, LiI 0.1 M, and 4-tertbutyl pyridine 0.5 M in 3-methoxypropionitrile, was introduced. Finally, the drilled holes were sealed with a microscope cover slide to avoid leakage of the electrolyte.

Preparation of Bpy3. A mixture of benzene-1,3,5-triol (153 mg, 1.21 mmol), 4-(bromomethyl)-4′-methyl-2,2′-bipyridine (1.00 g, 3.80 mmol), K_2CO_3 (1.00 g, 7.24 mmol), and a catalytic amount of 18-crown-6 were refluxed in acetone for 48 h. After cooling, the solvent was taken off under vacuum, water was added, and the solution was extracted with CH_2Cl_2. After drying with anhydrous sodium sulfate, the solvent was evaporated to dryness and the product was purified on a silica gel column using acetone as the mobile phase. The collected eluent was then evaporated to dryness to afford 350 mg of a white solid (43% yield). Mp 209–210 °C. ^{1}H NMR (300 MHz, $CDCl_3$) δ ppm: 2.35 (s, 9H), 5.03 (s, 6H), 6.2 (s, 3H), 7.05 (d, J = 6 Hz, 3H), 7.28 (d, J = 6 Hz, 3H), 8.16 (s, 3H), 8.35 (s, 3H), 8.45 (d, J = 3 Hz, 3H), 8.57 (d, J = 3 Hz, 3H). ^{13}C NMR (75 MHz, $CDCl_3$) δ ppm: 19.1, 66.4, 93.1, 116.8, 119.4, 119.9, 122.8, 144.8, 146.1, 146.9, 147.3, 153.5, 154.5, 158.1. ESI MS: m/z = 673.30 $[M + H]^+$, calcd for $C_{42}H_{36}N_6O_3$, 672.28.

(19) Kroeze, J. E.; Savenije, T. J. *Thin Solid Films* **2004**, *451–452*, 54–59.
(20) Savenije, T. J.; Warman, J. M.; Goossens, A. *Chem. Phys. Lett.* **1998**, *287*, 148–153.
(21) Senadeera, G. K. R.; Kitamura, T.; Wada, Y.; Yanagida, S. *Sol. Energy Mater. Sol. Cells* **2005**, *88*, 315–322.
(22) Nazeeruddin, M. K.; Kay, A.; Rodicio, I.; Humphry-Baker, R.; Muller, E.; Liska, P.; Vlachopoulos, N. *J. Am. Chem. Soc.* **1993**, *115*, 6382–6390.
(23) Klein, C.; Nazeeruddin, M. K.; Liska, P.; Di Censo, D.; Hirata, N.; Palomares, E.; Durrant, J. R.; Gratzel, M. *Inorg. Chem.* **2005**, *44*, 178–180.
(24) Wang, P.; Klein, C.; Humphry-Baker, R.; Zakeeruddin, S. M.; Gratzel, M. *J. Am. Chem. Soc.* **2005**, *127*, 808–809.
(25) Campbell, W. M.; Burrell, A. K.; Officer, D. L.; Jolley, K. W. *Coord. Chem. Rev.* **2004**, *248*, 1363–1379.
(26) Amadelli, R.; Argazzi, R.; Bignozzi, C. A.; Scandola, F. *J. Am. Chem. Soc.* **1990**, *112*, 7099–7103.
(27) Jang, S. R.; Vittal, R.; Lee, J. H.; Jeong, N.; Kim, K. J. *Chem. Commun.* **2006**, 103–105.
(28) Berg, K. E.; A, T.; Raymond, M. K.; Abrahamsson, M.; Wolny, J.; Redon, S.; Anderson, M.; Sun, L.; Styring, S.; Hammarstrom, L.; Toftlund, H.; Akermark, B. *Eur. J. Inorg. Chem.* **2001**, *101*, 1019–1029.
(29) Nazeeruddin, M. K.; Grätzel, M.; Rillema, D. P. *Inorg. Synth.* **2002**, *33*, 185–189.
(30) Will, G.; Boschloo, G.; Hoyle, R.; Rao, S. N.; Fitzmaurice, D. *J. Phys. Chem. B* **1998**, *102*, 10272–10278.
(31) Caspar, J. V.; Meyer, T. J. *J. Am. Chem. Soc.* **1983**, *105*, 5583–5590.

Preparation of Ru3. Bpy3 (88 mg, 0.13 mmol) and (4,4′-dc-bpy)$_2$RuCl$_2$ (350 mg, 0.53 mmol) were dissolved in 200 mL of 10/1 ethanol:water and refluxed under N_2 for 24 h. After cooling, the solvent was evaporated under vacuum and the crude solid was dissolved in a minimum amount of 40% tertra-butyl ammonium hydroxide in methanol. The solution was applied on a Sephadex LH-20 column using methanol as the eluting solvent. The major band was collected and the pH was adjusted to 2.0 by the addition of 2 M HCl. A dark red solid precipitated out which was collected by filtration and vaccuum-dried. This afforded the Ru3 dendrimer as the corresponding Cl^- salt (210 mg, 61%). ^{1}H NMR (300 MHz, DMSO) δ ppm: 2.51 (s, 9H), 5.35 (s, 6H), 6.62 (s, 3H), 7.38 (d, J = 6.0 Hz, 3H), 7.57 (m, J = 6.0 Hz, 3H), 7.59 (d, J = 6.0 Hz, 3H), 7.73 (d, J = 6.0 Hz, 3H), 7.86 (s, J = 5.4 Hz, 12H), 7.96 (d, J = 5.4 Hz, 12H), 9.02 (s, 3H), 9.12 (s, 3H), 9.28 (s, 12H). ^{13}C NMR (75 MHz, DMSO) δ ppm: 20.6, 78.9, 109.3, 113.2, 117.0, 120.8, 124.1, 126.9, 139.4, 150.7, 151.4, 152.7, 155.3, 156.2, 157.0, 158.0, 158.5, 159.0, 159.7, 164.8. Anal. Calcd for $C_{115}H_{87}N_{18}O_{27}Ru_3$: C, 56.23; H, 3.57; N, 10.26. Found: C, 56.03; H, 3.43; N, 10.03.

Preparation of Bpy$_2$OH. 5-Hydroxymethyl-benzene-1,3-diol (0.40 g, 3.12 mmol), 4-bromomethyl-4′-methyl-2,2′ bipyridine (2.00 g, 7.50 mmol), anhydrous K_2CO_3 (1.64 g, 120 mmol), and a catalytic amount of 18- crown-6 were refluxed in anhydrous acetone under N_2 atmosphere for 24 h. After cooling the solution was concentrated and then applied on a silica gel column. The column was flushed with acetone. The collected eluent was concentrated under vacuum followed by the addition of hexane to precipitate out a white solid that was collected by filtration and vaccuum-dried (1.27 g, 88% yield). Mp 106–108 °C. ^{1}H NMR (300 MHz, $CDCl_3$) δ ppm: 2.39 (s, 6H), 4.58 (d, J = 2.4 Hz, 2H), 5.09 (s, 4H), 6.50 (t, J = 1.1 Hz, 1 H), 6.59 (d, J = 1.1 Hz, 2H), 7.1 (d, J = 4.7 Hz, 2H), 7.33 (d, J = 4.7 Hz, 2H), 8.18 (s, 2H), 8.36 (s, 2H), 8.48 (d, J = 4.9 Hz, 2H), 8.60 (d, J = 4.9 Hz, 2H). ^{13}C NMR (75 MHz, $CDCl_3$) δ ppm: 31.0, 65.0, 68.0, 100.0, 101.4, 106, 119, 121.5, 122.1, 124.8, 143.8, 147.1, 148.9, 149.4, 155.6, 156.5, 159.6. ESI MS: m/z = 505.1 $[M + H]^+$, calcd for $C_{31}H_{28}N_4O_3$, 504.2.

Preparation of Bpy$_2$Br. Bpy$_2$OH (0.60 g, 1.19 mmol) and CBr_4 (1.50 g, 4.52 mmol) were dissolved in dry THF. The resulting solution was stirred under a N_2 atmosphere in an ice bath. After few minutes, Ph_3P (0.30 g, 1.17 mmol) was added and the reaction was left to stir for 24 h. The solvent was evaporated to dryness, and the product was purified on a silica gel column using acetone as the mobile phase. The collected eluent was then evaporated to dryness, and a white product was obtained (0.28 g, 50% yield). Mp 138–139 °C. ^{1}H NMR (300 MHz, $CDCl_3$) δ ppm: 2.38 (s, 6H), 4.21 (s, 2H), 5.08 (s, 4H), 6.35 (t, J = 1.1 Hz, J = 1.12 Hz, 1 H), 6.42 (d, J = 1.1 Hz, 2H), 6.96 (d, J = 4.6 Hz, 2H), 7.20 (d, J = 4.6 Hz, 2H), 8.03 (s, 2H), 8.12 (s, 2H), 8.30 (d, J = 4.6 Hz, 2H), and 8.5 (d, J = 4.6 Hz, 2H). ^{13}C NMR (75 MHz, $CDCl_3$) δ ppm: 24.1, 35.0, 72.1, 100.1, 106.0, 125.2, 125.3, 125.5, 125.7, 141.0, 149.1, 150.2, 151.0, 155.1, 155.2, 157.1, 162.1. ESI MS: m/z = 568.5 $[M + H]^+$, calcd for $C_{31}H_{27}N_4O_2Br$, 567.5.

Preparation of Bpy6. Bpy$_2$Br (1.00 g, 1.76 mmol), benzene-1,3,5-triol (70 mg, 0. 58 mmol), anhydrous K_2CO_3 (0.50 g, 3.57 mmol), and a catalytic amount of 18-crown-6 were refluxed in acetone under a N_2 atmosphere for 48 h. After cooling, the solution was concentrated and purified on a silica column using acetone as the mobile phase. The solvent was then evaporated and the white solid obtained was recrystallized from acetone/hexane (0.12 g, 13% yield). Mp dec 300 °C. ^{1}H NMR (300 MHz, $CDCl_3$) δ ppm: 2.35 (s, 18H), 4.71 (s, 6H), 5.07 (s, 12H), 6.15 (s, 3H), 6.51 (t, 3H), 6.63 (d, J = 3 Hz, 6H), 7.10 (d, J = 4 Hz, 6H), 7.30 (d, J = 4.9 Hz, 6H), 8.15 (s, 6H), 8.35 (s, 6H), 8.48 (d, J = 5.0 Hz, 6H), 8.58 (d, J = 5.0 Hz, 6H). ^{13}C NMR ($CDCl_3$): 20.8, 68.1, 69.5, 106.2, 118.5, 121.1, 121.7, 124.5, 139.5, 146.6, 147.8, 148.6, 149.1, 155.2, 156.1, 159.3, 160.0. ESI MS: m/z = 1586.8 $[M + H]^+$, calcd for $C_{99}H_{84}N_{12}O_9$, 1585.5.

Preparation of Ru6. Bpy6 (0.12 g, 0.076 mmol) and (4,4′-dc-bpy)$_2$RuCl$_2$ (0.40 g, 0.60 mmol) were refluxed in ethanol for 24 h. After cooling, the solvent was evaporated. The crude product was dissolved in 40% tetra-butyl ammonium hydroxide solution in methanol and applied on a Sephadex LH-20 column using methanol as the eluting solvent. The major band was collected, and the pH was adjusted to 2.0 by the addition of 2 M HCl. A dark red solid precipitated and was collected by filtration then vaccuum-dried. This afforded the **Ru6** dendrimer as the corresponding Cl^- salt (100 mg, 24% yield). ^{1}H NMR (300 MHz, DMSO) δ ppm: 2.30 (s, 18H), 4.98 (s, 6H), 5.27 (s, 12H), 6.30 (s, 3H), 6.7 (d, J = 1.2 Hz, 6H), 7.2 (s, 3H), 7.39 (d, J = 1.8 Hz, 12H), 7.53 (d, J = 2.1 Hz, 6H), 7.8 (m, 48H), 8.1 (s, 6H), 8.43 (d, J = 6 Hz, 12H), 8.62 (d, J = 6 Hz, 18H), 8.76 (s, 6H), 8.89 (s, 6H), 9.25 (s, 12 H). ^{13}C NMR (75 MHz, DMSO) δ ppm: 21.5, 65.1, 92.0, 98.4, 105.0, 118.2, 121.1, 122.0, 123.9, 124.9, 125.3, 137.5, 143.1, 146.8, 148.7, 150.2, 150.7, 153.4, 154.2, 155.0, 157.0, 162.8, 165.8. Anal. Calcd for $C_{243}H_{180}C_{112}N_{36}O_{57}Ru_6$: C, 52.61; H, 3.27; N, 9.09. Found: C, 52.20; H, 3.07; N, 8.90.

Results and Discussion

First and second generation dendrimers with 2,2′-bipyridyl units at the periphery (**Bpy3** and **Bpy6**) were prepared following the general procedure developed by Fréchet et al.,[32] where reacting the corresponding dendritic bromides with 1,3,5-benzene triol gave the desired metal-free dendrimers, Scheme 1. The ruthenium-based dendrimers, **Ru3** and **Ru6** (Scheme 1), were prepared by the complexation of (4,4′-dc-bpy)$_2$RuCl$_2$ and the respective metal-free dendrimer in a water/ethanol mixture under reflux for 24 h. The dendrimers were characterized by UV–vis, fluorescence, ^{1}H NMR, and ^{13}C NMR spectroscopy.

Photophysical Properties. Absorption and emission spectra of **Ru1**, **Ru3**, and **Ru6** were obtained in 1 M PBS buffer solution. Figure 1 shows the absorption spectra of the metallo-dendrimers and **Ru1** as a reference. The three complexes show broad absorption bands between 400 and 600 nm due to metal to ligand charge transfer (MLCT).[33] Compared to **Ru3** and **Ru6**, **Ru1** is slightly blue-shifted. This blue shift can be attributed to the difference in the substituents present at the 4,4′ positions of the bipyridine ligands.[34] In the UV region, both **Ru3** and **Ru6** show a strong absorption band at 306 nm that is due to an intraligand ($\pi-\pi^*$) charge transition that is assigned to the bipyridine ligands, while the blue-shifted spectrum of **Ru1** shows an absorption band at 302 nm. The molar extinction coefficient of the MLCT band at 478 nm for **Ru6** ($\epsilon = 9.5 \times 10^4$ M^{-1} cm^{-1}) is about 2 times greater than the molar extinction coefficient of **Ru3** ($\epsilon = 4.7 \times 10^4$ M^{-1} cm^{-1}) and 6 times higher than the reference compound **Ru1** ($\epsilon = 1.7 \times 10^4$ M^{-1} cm^{-1}). This increase in the molar extinction coefficient

(32) Grayson, S. M.; Frechet, M. J. *Chem. Rev.* **2001**, *101*, 3819–3867.
(33) Balzani, V.; Juris, A.; Venturi, M.; Campagna, S.; Serroni, S. *Chem. Rev.* **1996**, *96*, 759–833.
(34) Kalyanasundaram, K. *Coord. Chem. Rev.* **1982**, *46*, 159–244.

Scheme 1. Synthetic Scheme of the Two Dendrimers **Ru3** and **Ru6** and the Structure of **Ru1**[a]

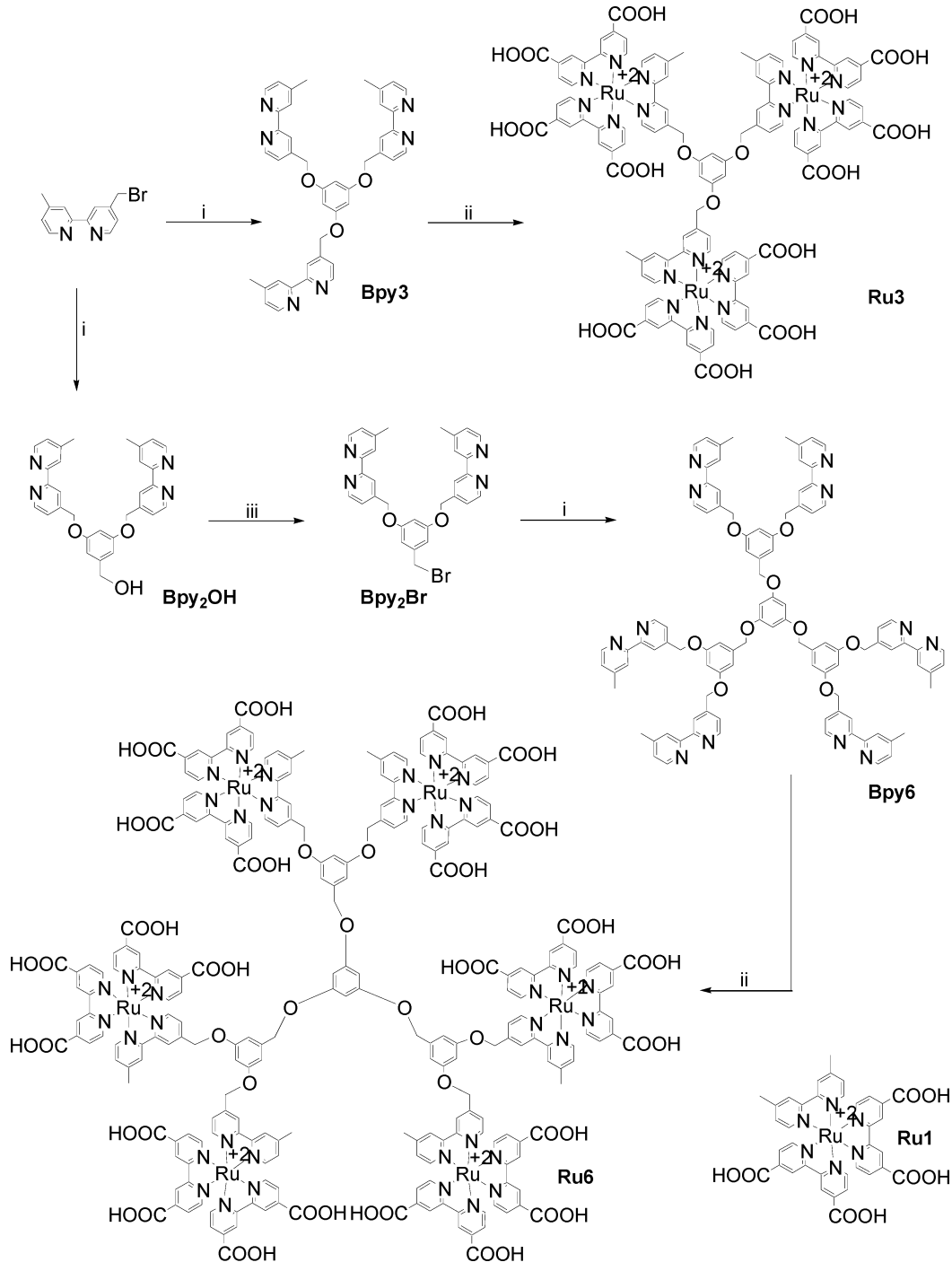

[a] (i) 1,3,5-Benzene triol, K_2CO_3, reflux in acetone. (ii) $(4,4'\text{-dc-bpy})_2RuCl_2$, reflux in ethanol/water. (iii) CBr_4 and PPh_3, in THF at RT.

is expected due to the increase in the number of the absorbing ruthenium moieties per dendrimer when going from **Ru1** to **Ru6**.

The emission spectra of **Ru1**, **Ru3**, and **Ru6** in 1 M PBS buffer are shown in Figure 2. The emission maxima are centered at 636, 630, and 628 nm, respectively. This blue shift in the emission spectra as one goes higher in dendrimer generation can be attributed to structural differences between the three compounds, where the sensitivity of the ruthenium chromophores to the dendritic backbone plays an important role in the emission properties of the three complexes. In other words, the dendrimer's arms may be playing a significant role in defining the solvent shell around the ruthenium moieties which in turn would result in such differences in the photophysical properties. In addition to this, a monotonic increase of the emission intensity was observed when going higher in dendrimer generation. The normalized emission decay profiles at room temperature for **Ru1**, **Ru3**, and **Ru6** are shown in Figure 3, and the emission lifetimes obtained from the deconvolution and least-squares fitting analysis are presented in Table 1. The emission lifetime was determined to be 300 ns for **Ru1**. However the

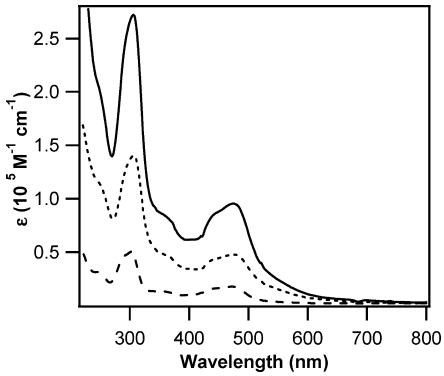

Figure 1. UV–vis absorption spectra of **Ru6** (solid), **Ru3** (dotted), and **Ru1** (dashed) in 1 M aqueous PBS buffer.

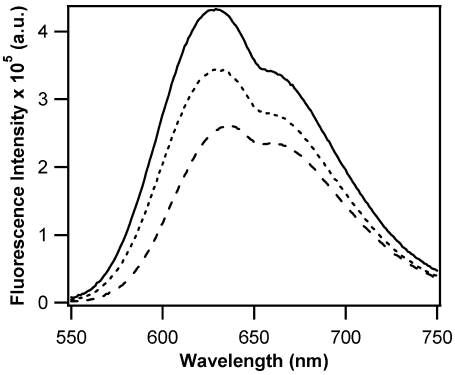

Figure 2. Steady-state emission spectra of **Ru6** (solid), **Ru3** (dotted), and **Ru1** (dashed) in 1 M aqueous PBS buffer, $\lambda_{ex} = 460$ nm.

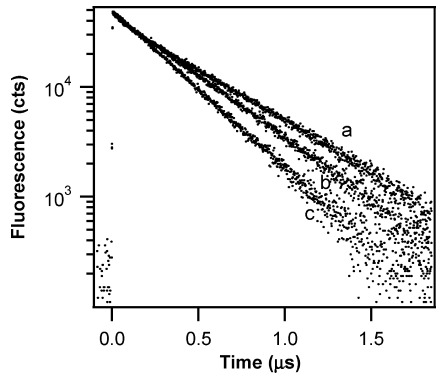

Figure 3. Lifetime emission spectra of (a) **Ru6**, (b) **Ru3**, and (c) **Ru1** in 1 M aqueous PBS buffer, $\lambda_{ex} = 460$ nm.

emission lifetime traces of **Ru3** and **Ru6** were best fitted by using a sum of two exponentials. The short-lived component ($\tau = 72$ and 60 ns for **Ru3** and **Ru6**, respectively) can be attributed to self-quenching of the pendant ruthenium moieties within a dendrimer that is in close proximity. As can be seen, the average emission lifetime increases monotonically when going from **Ru1** to **Ru6**, where an increase of 25% and 39% is calculated for **Ru3** and **Ru6** when compared to that of **Ru1**, respectively.

The absorption spectra of the three complexes **Ru1**, **Ru3**, and **Ru6** adsorbed on 8.0 μm thick TiO_2 nanocrystalline film are shown in Figure 4. The three adsorbed dyes were doped from 3 to 4 $\times$ 10^{-4} M solutions of **Ru1**, **Ru3** and **Ru6** employing the same conditions (1:1 methanol:water, pH 3.5). The absorption maximum of the three compounds on the oxide surface is around 475 nm, which is very similar to that in solution. However, the absorption band is relatively broad on the TiO_2 oxide surface, and the tail absorption extends up to 650 nm. Broadening of the absorption band is indicative of a charge transfer interaction between the ruthenium complexes and the oxide surface. Similar broadening of the absorption spectra has been observed for several sensitizers adsorbed on TiO_2 surfaces.[22,35] This may also be due to the change in the energy levels of the ground and excited states of the ruthenium moieties caused by adsorption. The difference in the absorption intensities of the three dyes adsorbed on the TiO_2 films indicates that there is a difference in the adsorption properties of the three compounds within the films. Compared to **Ru6** and **Ru1**, **Ru3** shows the highest absorption intensity in the MLCT region, where the **Ru3** film's absorption is 1.8 times higher than **Ru1** and 1.1 times higher than that of **Ru6**. This suggests that the **Ru3** film has a higher density of the adsorbed ruthenium moieties when compared to the **Ru1** and **Ru6** films.

Photocurrent–Voltage Characteristics of the Dendrimers Coated TiO_2 Electrodes. Figure 5 shows the current–voltage (*IV*) curves for 8.0 μm thick nanocrystalline TiO_2 solar cells sensitized with **Ru1**, **Ru3**, and **Ru6** dyes and measured at 25 °C with an area of 0.120 cm^2 and an irradiance of 100 mW cm^{-2}. It has been observed that the highest short circuit current density (J_{sc}) was obtained for the **Ru3** dye with a value of $J_{sc} = 5.52$ mA cm^{-2}. **Ru1** and **Ru6** gave a short circuit current density of $J_{sc} = 2.75$ and $J_{sc} = 2.50$ mA cm^{-2}, respectively. The open circuit voltages (V_{oc}) of the three dyes were close to each other giving $V_{oc} =$ 629, 626, and 608 mV for **Ru1**, **Ru3**, and **Ru6** respectively. The short-circuit photocurrent density (J_{sc}) and the open-circuit voltage (V_{oc}) values for each dye-coated TiO_2 electrode are reported in Table 2, in addition to the fill factors (ff) and the overall cell efficiencies (η). The **Ru3** sensitized solar cell gave the highest conversion efficiency corresponding to $\eta = 1.80\%$ with a fill factor of 0.52. The **Ru1** and **Ru6** sensitized solar cells showed lower conversion efficiencies corresponding to $\eta = 0.91$ and $\eta = 0.95\%$, respectively. From these results, we observe that the **Ru3** sensitized solar cell has shown an overall conversion efficiency around double that of the **Ru1**. The reasons behind this behavior may be explained in terms of the absorption properties of the particularly doped TiO_2 electrode, slower charge recombination processes due to the dendritic architecture, and/or an antenna effect. As it is shown in Figure 3, the **Ru3** film has a much higher absorbance in the visible region when compared to **Ru1**, especially in the red region of the absorption spectrum (470–650 nm). For example, at 550 nm a **Ru3** film absorbs an additional 35% of the incident light when compared to a **Ru1** film of the same thickness. In addition to this, an electron transfer reaction (ET) can take place across the perimeter within the dendrimer between an oxidized (+3) and unoxidized (+2) ruthenium moieties right after the electron injection into the TiO_2 conduction band. Theory and experiment have shown that such self-exchange ET rates are comparable to those occurring between redox

(35) Vinodgopal, K.; Hua, X.; Dahlgren, R. L.; Lappin, A. G.; Patterson, L. K.; Kamat, P. V. *J. Phys. Chem.* **1995**, *99*, 10883–10889.

Table 1. Photophysical Properties of **Ru1**, **Ru3**, and **Ru6** in Solution

	absorption λ, nm (ϵ, 10^5 M^{-1} cm^{-1})[a]	emission λ, nm[a,b]	lifetime $\tau(I)$, ns[a,b]	quantum yield Φ[a]
Ru1	302 (0.50), 475 (0.17)	636	300	0.010
Ru3	306 (1.38), 478 (0.47)	630	72 (0.06), 395 (0.94)	0.013
Ru6	306 (2.72), 478 (0.95)	628	60 (0.14), 475 (0.86)	0.016

[a] Measured in 1 M aqueous PBS buffer. [b] $\lambda_{ex} = 460$ nm.

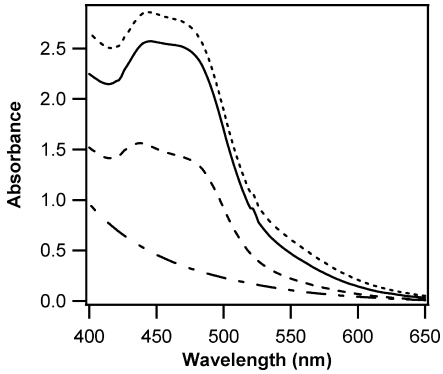

Figure 4. Uncorrected UV–vis absorption spectra of **Ru6** (solid), **Ru3** (dotted), and **Ru1** (dashed) adsorbed on 8.0 μm thick nanocrystalline TiO_2 film (dashed-dotted).

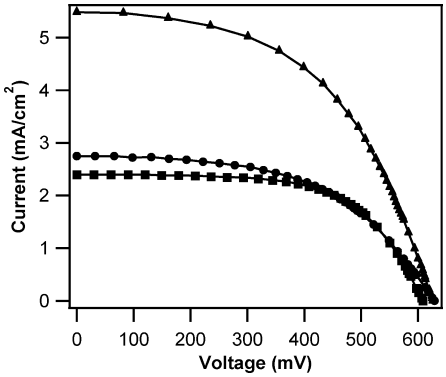

Figure 5. Photocurrent–voltage curves of solar cells based on (▲) **Ru3**, (●) **Ru1**, and (■) **Ru6**, measured under an illumination of 100 mW cm^{-2}. The active cell area is 0.120 cm^2.

Table 2. Photovoltaic Performance of DSSCs with **Ru1**, **Ru3**, and **Ru6** as Sensitizers

	V_{oc}, mV	J_{sc}, mA cm^{-2}	ff	η%[a]
Ru1	629	2.75	0.53	0.91
Ru3	626	5.52	0.52	1.80
Ru6	608	2.50	0.62	0.95

[a] Measured with 0.05 M I_2, 0.1 M LiI, and 0.5 M 4-tertbutyl pyridine in 3-methoxypropionitrile as the corresponding electrolyte under 100 mW$\cdot$ cm^{-2} illumination.

centers in contact.[36] Such an ET reaction may result in a better charge separation and thus slower charge recombination processes between the TiO_2 and the oxidized ruthenium center. Moreover, one cannot exclude exciton hopping between the ruthenium centers within the dendrimer framework, which in turn may be viewed as an antenna effect similar to that seen by O'Regan and Grätzel[10] and Amadelli et al.[26] On the other hand, **Ru6** did not show any significant enhancement in the conversion efficiency even though the **Ru6** film has a much higher absorption in the red part of the visible region than the **Ru1** film. Such a discrepancy can

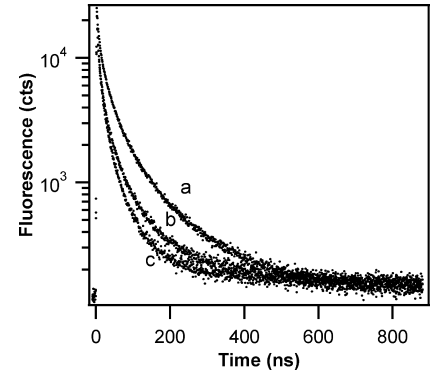

Figure 6. Lifetime emission spectra of (a) **Ru6**, (b) **Ru3**, and (c) **Ru1** adsorbed on 8.0 μm thick nanocrystalline TiO_2 film, $\lambda_{ex} = 460$ nm.

be attributed to the fact that for an efficient electron injection to take place from the excited ruthenium moiety to the TiO_2, the ruthenium moiety has to be anchored through its dicarboxy-bipyridine ligand(s) to the TiO_2; that is, for **Ru6**, at least six carboxylic acid moieties on the six different ruthenium centers have to be anchored at the same time. Such a requirement would be more difficult to satisfy than that of the **Ru3** case due to geometrical factors. Recently, Bell et al.[37] have confirmed that electron injection from $(bpy)_2Ru(dcbpy)$ to mesoporous TiO_2 proceeds with rates exceeding 10^{13} s^{-1} and that the residual slower processes (>1 ns) are attributed to imperfectly bound dye molecules. Therefore, we decided to performed TCSPC measurements on the three **Ru1**, **Ru3**, and **Ru6** TiO_2 films to compare the amount of the weakly bound ruthenium moieties between the three different films. Figure 6 shows the normalized emission decay profiles for the **Ru1**, **Ru3**, and **Ru6** TiO_2 films. The emission decays of the three films deviate from the single-exponential behavior, probably due to the existence of multiple injection/adsorption sites on the TiO_2 surface. The decay curves were analyzed and fitted by using a sum of four exponentials. In the literature, decay curves of analogous poly(pyridyl ruthenium) complexes adsorbed on semiconductor oxide films have been analyzed by using a sum of up to four exponentials, and the reported results are very similar to our **Ru1** and **Ru3** case.[35,37,38] Table 3 summarizes the decay lifetimes and the pre-exponential factors for each compound. The main important result obtained from Table 3 is that the lifetimes and the pre-exponential factors of each decay component are very similar within the experimental error for **Ru1** and **Ru3**. However, for the **Ru6** case the pre-exponential factors are very different from that of **Ru1** and **Ru3** in addition to the lifetime components, where the long-lived components (τ_3 and τ_4) constitute more than 37% of

(36) Amatore, C.; Bouret, Y.; Maisonhaute, E.; Goldsmith, J. I.; Abruna, H. D. *Chem. Eur. J.* **2001**, *7*, 2206–2226.

(37) Bell, T. D. M.; Pagba, C.; Myahkostupov, M.; Hofkens, J.; Piotrowiak, P. *J. Phys. Chem. B* **2006**, *110*, 25314–25321.

(38) Hashimoto, K.; Hiramoto, M.; Kajiwara, T.; Sakata, T. *J. Phys. Chem.* **1988**, *92*, 4636–4640.

Table 3. Lifetime and Relative Weights of Pre-Exponential Factors of the Emission from **Ru1**, **Ru3**, and **Ru6** Adsorbed on Nanocrystalline TiO_2

	τ_1, ns (I_1, %)	τ_2, ns (I_2, %)	τ_3, ns (I_3, %)	τ_4, ns (I_4, %)
Ru1[a]	2.8 (66.4)	13 (25.1)	40 (7.9)	172 (0.6)
Ru3[a]	2.5 (64.4)	11 (24.4)	40 (9.8)	144 (1.4)
Ru6[a]	4.1 (37.9)	17 (24.6)	50 (28.2)	152 (9.3)

[a] $\lambda_{ex} = 460$ nm and $\lambda_{em} = 630$ nm under aerobic conditions.

the decay profile, whereas in the case of **Ru1** and **Ru3** τ_3 and τ_4 constitute less than 11% of the whole decay profile. The long-lived component can be attributed to unanchored ruthenium moieties and/or nonadsorbed molecules that are sequestered within the interstitial space of the TiO_2 film.[37,39] Therefore, it becomes clear that in the **Ru6** case not all of the ruthenium moieties within a dendrimer molecule and/or not all of the **Ru6** dendrimer molecules are anchored to the TiO_2 which in turn results in smaller cell efficiencies when compared to **Ru3**.

Conclusions

We were able to synthesize first- and second-generation dendrimers with ruthenium polypyridyl moieties at the periphery. When compared with $(4,4'\text{-dc-bpy})_2\text{Ru(dm-bpy)}$ (**Ru1**), the emission quantum yield increases and the emission maxima blue-shifts as the dendrimer generation increases. This was attributed to the sensitivity of the ruthenium chromophores to the dendritic backbone which affects the excited-state energy levels and in turn has a great influence on the emission maxima and the radiative and nonradiative decay rates. **Ru3** and **Ru6** were especially designed to study the dendritic effect on dye sensitized solar cells. **Ru1**, **Ru3**, and **Ru6** have been successfully tested as sensitizers on nanocrystalline TiO_2 cells. The **Ru3** based DSSC showed the highest photon-to-current conversion efficiency of $\eta = 1.80\%$ when compared to **Ru1** and **Ru6**. The higher efficiency of the **Ru3** based DSSC when compared to **Ru1** and **Ru6** may be attributed to higher light harvesting properties in the red region of the visible absorption, dendritic effect, and/or an antenna effect. The **Ru6** based DSSC gave a similar DSSC efficiency ($\eta = 0.95\%$) to **Ru1** but smaller than **Ru3**. This was attributed to inefficient anchoring of all of the ruthenium chromophores to the TiO_2, and this was evident from the analysis of the lifetime emission measurements of the **Ru6** film. We are currently working on synthesizing a first generation dendrimer with **N3** analog moieties at the periphery and studying its efficiency as a DSSC dye.

Acknowledgment. This work was supported by the University Research Board (URB) at the American University of Beirut (AUB) and the Lebanese National Council for Scientific Research (LNCSR).

IC702432U

(39) Richard, W.; Fessenden, W.; Kamat, P. V. *J. Phys. Chem.* **1995**, *99*, 12902–12906.